A Feasible Zone Analysis Method with Global Partial Load Scanning for Solving Power Flow Coupling Models of CCHP Systems

Pohan Chen, Kai Sun, *Senior Member*, *IEEE*, Chenghui Zhang, *Senior Member*, *IEEE*, and Bo Sun

Abstract—Heat exchanger systems (HXSs) or heat recovery steam generators (HRSGs) are commonly used in 100 kW to 50 MW combined cooling, heating, and power (CCHP) systems. Power flow coupling (PFC) is found in HXSs and is complex for researchers to quantify. This could possibly mislead the dispatch schedule and result in the inaccurate dispatch. PFC is caused by the inlet and outlet temperatures of each component, gas flow pressure variation, conductive medium flow rate, and atmosphere condition variation. In this paper, the expression of PFC is built by using quadratic functions to fit the nonlinearity of thermal dynamics. While fitting the model, the environmental condition needs prediction, which is calculated using phase space reconstruction (PSR) Kalman filter. In order to solve the complex quadratic dispatch model, a hybrid following electricity load (FEL) and following thermal load (FTL) mode for reducing the dimension of dispatch model, and a feasible zone analysis (FZA) method are proposed. As a result, the PFC problem of CCHP system is solved, and the dispatch cost, investment cost, and the maximum power requirements are optimized. In this paper, a case in Jinan, China is studied. The PFC model is proven to be more precise and accurate compared with traditional models.

Index Terms—Combined cooling, heating, and power (CCHP) system, renewable energy source (RES), load prediction, operation strategy, exergy and energy analysis, power flow coupling (PFC) model.

I. INTRODUCTION

COMBINED cooling, heating, and power (CCHP) systems have attracted researchers' attention because of the high efficiency and low environmental impact [1]. Differ-ent topologies of CCHP systems have been considered in order to improve the performance and make full use of renewable energy sources (RESs).

Heat exchanger systems (HXSs) are commonly used for multiple strategies in small-scale, medium-scale, and large-scale CCHP systems. HXSs can improve the total capacity of the fuel consumption, with which the systems could completely recover the waste heating [1]. In [2], three HXSs are used to adjust different seasonal demands of users. Heat recovery steam generators (HRSGs) and HXSs function as the waste heating collectors and heating flow generators in high-speed railway stations, respectively. Both of them function as the adjustment components for heating-electricity load ratio [3]. These applications of the HXSs improve the performance of CCHP systems but bring complex nonlinear thermodynamics.

There are four main categories in thermodynamic modeling [4], including the lump modeling approach [5], the moving boundary approach, the tube-by-tube approach [6], and the segment-by-segment approach [4], [7]. All the above four main categories prove that the models of HXSs are nonlinear. The dispatch models of CCHP systems are usually linear [8]. In most cases, these differences are neglected.

Researches show that the HXSs have multiple energy coupling loops [9], namely power flow coupling (PFC). It is defined as when one state of a single component in HXS changes, the independent parameters of other components would be possibly influenced to be changed, resulting in dispatch deviations.

PFC is not yet being considered in the dispatch models of CCHP systems and the above common facts about PFC are neglected in former CCHP researches. A CCHP dispatch model considering PFC has to be proposed.

Firstly, in order to precisely build the PFC models, efficient data should be prepared. A precise prediction of RESs, CCHP loads, and environmental factors (humidity and temperature) is proposed as a data backup of PFC models [9]. After the precise prediction, the model is built according to the basic laws of thermodynamics inside the HXSs [10].

Secondly, due to the nonconvexity of PFC models, simplifying methods with few hypotheses need to be introduced to solve PFC models. The following load mode is used to simplify the calculation when solving PFC models. Two of the most common strategies are recognized as the following thermal load (FTL) mode and the following electricity load

P. Chen and K. Sun (corresponding author) are with the Department of Electrical Engineering, Tsinghua University, Beijing, China (e-mail: chenbh17@mails.tsinghua.edu.cn; sun-kai@mail.tsinghua.edu.cn).

C. Zhang and B. Sun are with the School of Control Science and Engineering, Shandong University, Jinan, China (e-mail: zchui@sdu.edu.cn; sunbo@sdu.edu.cn).

(FEL) mode. A hybrid FEL and FTL (FHL) mode is used in CCHP system recently and its impact is analyzed in [11]. In addition, the best operation strategy depends on the choice of the incentive policies. However, the FHL mode is the most suitable when there is no incentive policy [12]. The above researches prove that the following load modes are effective to reduce the dimensions of the dispatch model.

Thirdly, the algorithm needs to be improved because most general algorithms are not able to solve quadratic models. The genetic algorithm (GA) and its improved method are used in [1], [9], [13] to solve the optimal planning or dispatch of CCHP systems. Mixed-integer linear programming (MILP), as a precise optimal algorithm, is also used in many CCHP cases [8]. In a common view, programming algorithms including MILP, mixed-integer programming (MIP), and quadratic constraint programming (QCP) have more merits in precise calculation, but are less flexible in the adaptation of complex models. While intelligent algorithms such as GA, particle swarm optimization (PSO), and annealing algorithm (AA) can solve complex models with higher-scale of non-linearity, but their optimal solutions are less convincing.

The remainder of this paper is organized as follows. In Section II, the description of CCHP system and the corresponding methods are presented. In Section III, the optimization method is introduced. A case study is presented in Section IV. Statistic results are shown in Section V. In Section VI, significant conclusions of the proposed method are drawn.

II. DESCRIPTION AND MODELING

The topologies of RES system and CCHP system are shown in Fig. 1, where the RES system comprises wind tur-

bine (WT), photovoltaic (PV), and fuel cells (FCs), and the CCHP system comprises micro gas turbine (MGT), gas-fired boiler (GF), compress chiller (COM), heating exchanger (HX), and absorption chiller (ABS). In this section, the model of CCHP system is proposed according to [8].
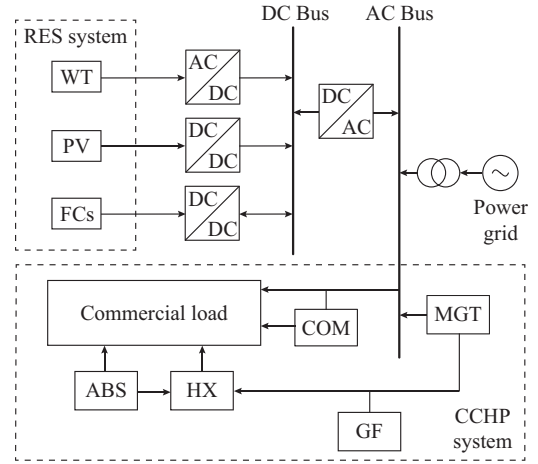

Fig. 1. Topologies of RES system and CCHP system.

A. MGT and HXS Models

The CCHP system is further divided into two parts, namely the MGT system and HXS system [10], as shown in Fig. 2. The input air represented by Flow 1 functions as the supporting air of combustion, which is compressed and injected to the turbine. The fuel flow represented by Flow 2 contributes the system with chemical power. The fuel flow raises the fluid temperature and helps acceleration. In HXS, the cycle includes water flow and gas flow, namely w_1-w_4 and g_1-g_4, respectively.
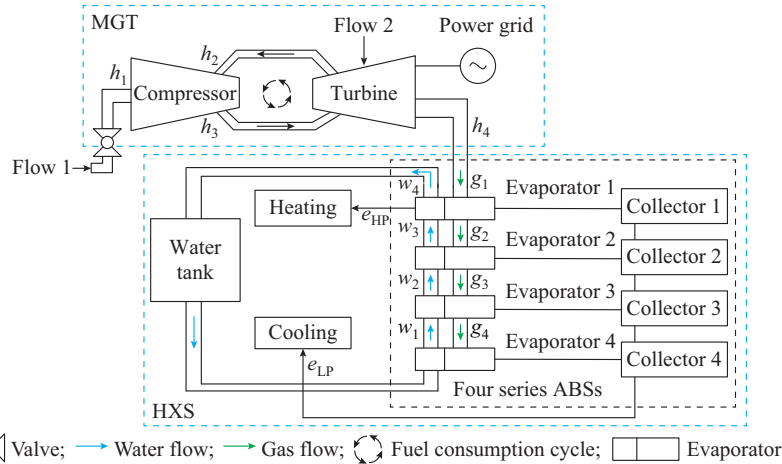

Fig. 2. MGT and HXS in CCHP system.

The efficiency of compressor η_c is expressed as:

$$\eta_c = 1 - \left(0.04 + \frac{\gamma_c - 1}{150}\right) \tag{1}$$

where γ_c is the pressure ratio of compressor.

The required work of compressor is calculated as:

$$\dot{W}_c = \dot{m}_c(1 + \omega_1)(h_2 - h_1) \tag{2}$$

where $\dot{W}_c$ is the rate of the required work, also regarded as the input power of compressor; $\dot{m}_c$ is the flow rate of compressor gas; ω_1 is the humidity ratio; and h_1 and h_2 are the enthalpy of the medium at the inlet and outlet of compressor, respectively.

The heating energy of the fuel consumption cycle is expressed as:

$$\dot{W}_T = \dot{m}_f(1+\lambda)(h_3 - h_2) \qquad (3)$$

where $\dot{W}_T$ is the thermal power of turbine; $\dot{m}_f$ is the flow rate of fuel; λ is the fuel-to-air ratio; and h_3 is the enthalpy of the combusting cycle.

The output power of turbine is calculated as:

$$\dot{W}_t = \dot{m}_t(h_4 - h_3) \qquad (4)$$

where $\dot{m}_t$ is the mass flow rate of turbine gas; and h_4 is the enthalpy at the inlet of the four series ABSs.

The power to the power grid $\dot{W}_{Grid}$ is simply regarded as the subtraction of $\dot{W}_t$ and $\dot{W}_c$, which is expressed as:

$$\dot{W}_{Grid} = \dot{W}_t - \dot{W}_c \qquad (5)$$

B. Principles of MGT and HXS

Figure 2 also includes four series ABSs, water tanks, and cooling and heating equipment. These components obey the exergy balance rule.

The exergy balance equation and the mass balance equation for a steady system are given as:

$$\begin{cases} \dot{E}_W = \sum_{i=1}^{n} \dot{E}_Q^i + \sum \dot{m}_{in} e_{in} - \sum \dot{m}_{out} e_{out} - \dot{E}_D \\ \sum \dot{m}_{in} - \sum \dot{m}_{out} = 0 \end{cases} \qquad (6)$$

where $\dot{E}_W$ is the work of each component; $\dot{E}_Q^i$ is the thermal consumption of the ith component; n is the number of components; $\sum \dot{m}_{in} e_{in}$ and $\sum \dot{m}_{out} e_{out}$ are the input and output work, respectively, $e_{out} = \{e_{LP}, e_{HP}\}$, $\dot{m}_{in}$ and $\dot{m}_{out}$ are the input and output mass flow rates, respectively; and $\dot{E}_D$ is the nominal work.

The exergy of medium flow e_x is calculated as:

$$e_x = (h_x - h_0) - T_0(s_x - s_0) \qquad (7)$$

where s_x is the specific entropy of the medium flow, $x = 1, 2, 3, 4$; h_0, T_0, and s_0 are the initial temperature, enthalpy, and specific entropy, respectively. The detail enthalpy calculation of four series ABSs is shown in [10].

C. Environmental Condition Prediction

When calculating (6), the temperature, pressure, and moisture of the inlet and outlet are required. However, in order to improve the dynamic performance of the CCHP system, it is necessary to use the prediction data of the above variables in advance, rather than the historical data.

Compared with other methods, the Kalman filter has advantages in predicting CCHP loads and RESs at the same time. However, the Kalman filter needs the sequences with more dimensions to ensure its accuracy. The sequences for predicting CCHP loads and RESs have limited dimensions. In order to have a precise prediction, the dimensions of input sequences have to be increased.

Tokens theorem of embedding reveals that, when enough dimensions are embedded, $m \geq 2D+1$ should be satisfied, where m is the number of the embedded dimensions; and D is the number of the dynamic system dimensions [14].

This procedure is regarded as the phase space reconstitution (PSR) [14]. The PSR theory shows that if the number of dimension is satisfied, the sequence should be expressed as:

$$X = [X_1, X_2, ..., X_i, ..., X_t] \qquad (8)$$

where $X_i = \{x_i, x_{i+t}, ..., x_{i+(m-1)t}\}$.

The system state is rearranged in the matrix X and sent to the Kalman filter. The flow chart of Kalman filter is shown in Fig. 3, where Φ is the state transfer matrix; ω is the process noise vector; T is the impel transfer matrix; Z is the dimensional observation vector; H is the transfer matrix of prediction output; K is the Kalman gain; and k is the order of Kalman cycles.
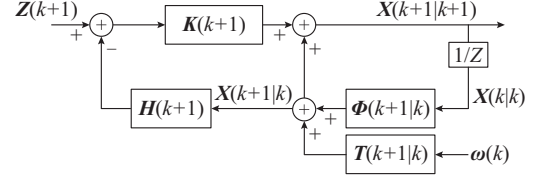

Fig. 3. Flow chart of Kalman filter.

D. Objective Function

A hybrid objective function considering the area and the operation cost is proposed in this section. Each objective function is evaluated separately. The function of annual total cost (ATC) of CCHP system is expressed as:

$$ATC = Cost_C + Cost_M + Cost_{Fuel} + Cost_{Grid} + Cost_R \qquad (9)$$

where ATC is the annual total cost; and $Cost_C$, $Cost_M$, $Cost_{Fuel}$, $Cost_{Grid}$, and C_R are the capital cost, maintenance cost, fuel cost, electricity cost, and replacement cost, respectively.

The capital cost $Cost_C$ is from initializing the CCHP system, which is expressed as:

$$Cost_{C,j} = Cap_j \cdot Cost_{U,j} \qquad (10)$$

where Cap_j is the capacity of installing component j; and $Cost_{U,j}$ is the unit cost of component j.

The maintenance cost $Cost_M$ is evaluated by:

$$Cost_M = Cost_{M,1} \frac{1+f}{i-f}\left[1 - \left(\frac{1+f}{1+i}\right)^{y^{max}}\right] \qquad (11)$$

where $Cost_{M,1}$ is the first-year maintenance cost; f is the inflation rate; y^{max} is the maximum operation year; and i is the depreciation rate.

The electricity cost $Cost_{Grid}$ and the fuel cost $Cost_{Fuel}$ are expressed as:

$$Cost_{Grid} = Price_{Grid} \sum_{t=1}^{n} E_{Grid,t} \qquad (12)$$

$$Cost_{Fuel} = Price_{Fuel} \sum_{t=1}^{n} (F_{MGT,t} + F_{GF,t}) \qquad (13)$$

where $Price_{Grid}$ and $Price_{Fuel}$ are the unit prices of electricity from power grid and fuel, respectively; $E_{Grid,t}$ is the electricity from power grid at time t; and $F_{MGT,t}$ and $F_{GF,t}$ are the fuel consumptions of MGT and GF at time t, respectively.

The replacement cost $Cost_R$ is expressed as:

$$Cost_R = Cap_j \cdot Cost_{U,j} \sum_{y=1}^{N_j} \frac{1}{\left(\frac{1+f}{1+r}\right)^y} \quad \forall y = 1, 2, ..., N_j \qquad (14)$$

where r is the annual interest rate; y is the operation year of CCHP system; and N_j is the maximum operation year of component j.

E. PFC Models

In this section, a quadratic dispatch model is built to quantify PFC models. Compared with the linear dispatch models proposed in [8], the proposed nonlinear PFC model is more accurate.

Firstly, few conclusions of [10] are mentioned to simplify the ideal system state when controlling the CCHP system. The experiment shows that the MGT and HXS reach their highest efficiencies when $\gamma_c = 14$. Thus, we keep γ_c unchanged when controlling the CCHP system.

Moreover, we need to control the cooling, heating, and power outputs of the CCHP system, respectively. Varying the low-pressure pinch point or pressure would change the cooling output without changing the heating or power output, while varying the high-pressure pinch point or pressure would change both heating and cooling outputs without changing the power output. The power output could be adjusted by increasing or decreasing the turbine inlet temperature (TIT), but it could change the cooling and heating outputs simultaneously.

Obviously, the above conclusions reveal a coupling relationship among the three outputs. For example, when the TIT changes from 1300 K to 1400 K, the power output changes from 19.23 MW to 23.64 MW; meanwhile, the heating output changes from 24.65 MW to 31.25 MW, and the cooling output changes from 6.96 MW to 4.51 MW. Obviously, if we need to enhance the power output of the CCHP system, a correction for heating and cooling is required. According to the above results, the power of PFC models are assumed to be between 1% and 5% of the total system power.

The PFC models contain five dispatch variables to determine a unique operation point (or the so-called dispatch state), which includes the electricity from MGT E_{MGT}, the heating from GF H_{GF}, the electricity from power grid E_{Grid}, the cooling from ABS C_{ABS}, and the cooling from COM C_{COM}. The first stage of the operation is to solve the optimized operation point of the CCHP system in an hour.

The operation point is expressed as follows.

1) Power Balance

$$E_{RES} + E_{Grid} + \eta_{MGT,E} F_{MGT} = E_{Load} + E_{Consume} \tag{15}$$

where E_{RES} is the electricity from RES system; E_{Load} is the requirement of electricity load; $E_{Consume}$ is the electricity consumption of HRSG to generate heating and cooling; F_{MGT} is the fuel consumption of MGT; and $\eta_{MGT,E}$ is the efficiency of fuel-to-electricity in the MGT.

2) Heating Balance

$$\eta_{MGT,H} F_{MGT} + H_{GF} = H_{Load} + H_{Consume} + H_{PFC} \tag{16}$$

where H_{Load} is the requirement of heating load; $H_{Consume}$ is the heating consumption of HRSG to generate cooling; $\eta_{MGT,H}$ is the efficiency of fuel-to-heating in the GF; and H_{PFC} is the heating loss of PFC during the generation, which is related to the variation of electricity and cooling.

3) Cooling Balance

$$C_{ABS} + C_{COM} = C_{Load} + C_{PFC} \tag{17}$$

where C_{Load} is the requirement of cooling load; and C_{PFC} is the cooling loss of PFC during the generation, which is related to the variation of heating and electricity.

4) PFC

In Section I, PFC is defined as: when one state of a single component in HXS changes, the independent parameters of other components would be possibly influenced to be changed, resulting in dispatch deviations.

The PFC is a product of two decision variables, which is expressed as:

$$H_{E,PFC} = \frac{E_{MGT,t+1} - E_{MGT,t}}{E_{MGT,t}} H_{GF,t+1} \tag{18}$$

$$C_{H,PFC} = \frac{H_{GF,t+1} - H_{GF,t}}{H_{GF,t}} C_{ABS,t+1} \tag{19}$$

$$C_{E,PFC} = \frac{E_{MGT,t+1} - E_{MGT,t}}{E_{MGT,t}} C_{ABS,t+1} \tag{20}$$

where $H_{E,PFC}$, $C_{H,PFC}$, and $C_{E,PFC}$ are the PFC of electricity and heating, the PFC of heating and cooling, and the PFC of electricity and cooling, respectively.

We assume that the power at time t is detectable, and the power at time $t+1$ is to be dispatched. Thus, the PFC model is a product of two decision variables. The first parts of (18)-(20) represent the power changes of the initial PFC components during the dispatch period $[t, t+1]$, and the second parts represent the power of the response components. For instance, $H_{E,PFC}$ is explained as the power change of GF caused by per-unit power change of the MGT. Similar definition is suitable for $C_{H,PFC}$ and $C_{E,PFC}$.

III. OPTIMIZATION METHOD

There are totally three constraint equations and five decision variables, and the feasible zone analysis (FZA) method is based on the coordinate of three decision variables F_{MGT}, E_{Grid}, and E_{COM}. The rest two decision variables H_{GF} and C_{ABS} are expressed in equivalence with partial load between FTL mode and FEL mode. Thus, the FHL mode is proposed to reduce the dispatch model by two dimensions.

In this section, the global variable $K\%$ is defined as the ratio of FTL to FEL. As shown in Fig. 4, the system is operating in the full FTL mode and full FEL mode when $K\% = 0\%$ and $K\% = 100\%$, respectively.

FTL   FEL
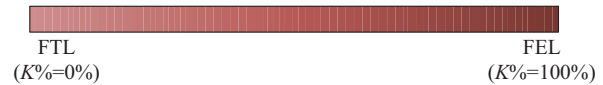($K\% = 0\%$)   ($K\% = 100\%$)

Fig 4.   Ratio of FTL to FEL.

When $K\% = 0\%$, it is obvious that the thermal energy is more expensive. Thus, it is cheaper to generate cooling by using electricity. Under this condition, the heating load is fully supplied by the MGT, the cooling load is fully supplied by the COM, and the insufficient electricity is supplied from the power grid.

To conclude, when the ratio of FTL to FEL is at $K\%$, $K\%$

of the electricity load and cooling load are satisfied by MGT and ABS, respectively. Meanwhile, $(100\% - K\%)$ of the electricity load and cooling load are satisfied by power grid and COM, respectively.

When $K\%$ is determined, two of the above five variables are replaced with certain values, so it is used to reduce dispatch state from 5-dimension to 3-dimension. If we scan $K\%$ from 1% to 100%, it is possible to obtain an optimal result with a set of 3-dimension images.

In this paper, a 3-dimension coordinate with x-axis for F_{MGT}, y-axis for E_{Grid}, and z-axis for E_{COM}, is constructed to illustrate the feasible analysis. The system feasible points (FPs) in full FTL mode ($K\%=0$) and 50% FTL mode ($K\%=50\%$) are shown in Figs. 5 and 6, respectively.
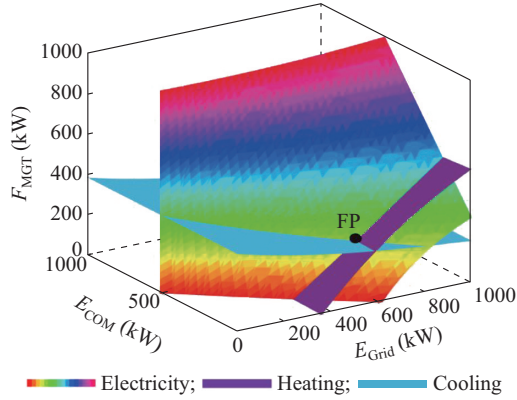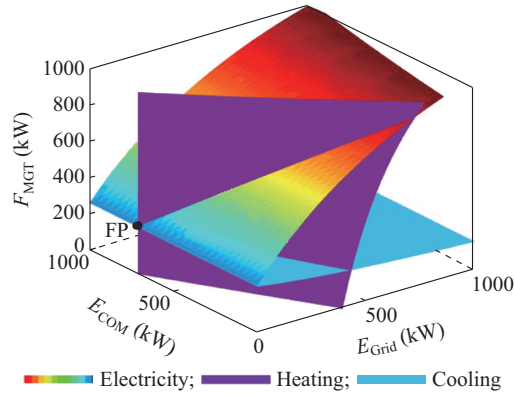

Fig 5.   FP in full FTL mode.

Fig 6.   FP in 50% FTL mode.

The minimum electricity generation is fixed on the electricity curved surface. Obviously, the minimum heating generation and cooling generation can also be determined. The intersection of the three curved surfaces is assumed as the FP.

The FP contains lower values of decision variables for F_{MGT}, E_{Grid}, and E_{COM}. The solution for two hidden decision variables H_{GF} and C_{ABS} are expressed as:

$$H_{GF} = \alpha_{GF} F_{GF}^2 + \beta_{GF} F_{GF} + \delta_{GF} = K\% \times H_{Load} \qquad (21)$$

$$C_{ABS} = COP \cdot H_{EXC} = \beta_{ABS} H_{EXC} + \delta_{ABS} = K\% \times C_{Load} \qquad (22)$$

where COP is the coefficient of performance, which represents the efficiency of cooling; H_{EXC} is the heating consumption of the ABS; and α_{GF}, β_{GF}, δ_{GF}, β_{ABS}, and δ_{ABS} are the fitting parameters.

Obviously, in a dispatch schedule, each $K\%$ from 0% to 100% corresponds to an FP. The optimization of dispatch schedule is equal to finding the optimal FP and $K\%$ by using the FZA method.

IV. CASE STUDY

A. Research Sample

A typical dispatch schedule of CCHP system in March in Jinan, China is studied in this section. The monthly climate monitoring is uploaded hourly, and there are $31 \times 24 = 744$ monitoring points in total. To examine the accuracy of the proposed method, the first 15-day data are used as the known database, and the late 16-day data are detected and optimized by the proposed method, which includes $16 \times 24 - 1 = 383$ points. The Pearson correlation results of load and RES prediction are shown in Table I.

TABLE I
PEARSON CORRELATION RESULTS OF LOAD AND RES PREDICTION

Item	Pearson correlation						
	CL	EL	HL	WS	SI	HU	TE
CL	1.00	0.45	−0.15	0.09	0.65	−0.54	0.82
EL	0.45	1.00	−0.19	0.17	0.56	−0.26	0.55
HL	−0.15	−0.19	1.00	−0.04	−0.24	0.21	−0.13
WS	0.09	0.17	−0.04	1.00	0.09	0.04	0.08
SI	0.65	0.56	−0.24	0.09	1.00	−0.43	0.66
HU	−0.54	−0.26	0.21	0.04	−0.43	1.00	−0.46
TE	0.82	0.55	−0.13	0.08	0.66	−0.46	1.00

Note: CL represents the cooling load; EL represents the electricity load; HL represents the heating load; WS represents the wind speed; SI represents the solar irradiance; HU represents the humidity; and TE represents the temperature.

It can be observed that the wind speed is almost not related to other parameters, so that the prediction is divided into the Kalman filter prediction with the wind speed and the Kalman filter prediction with other parameters.

B. Demonstration of FZA Method

According to the prediction result, the proposed FZA method is used to optimize the operation point and the dispatch schedule.

The operation power of components in the 251st interval of the total 383 hours is shown in Fig. 7. In this interval, there are 73 FPs and each FP corresponds to a certain $K\%$. The operation cost of the system in the 251st interval is shown in Fig. 8, and the minimum operation cost is ¥1383.887, which corresponds to the 35th FP ($K\%=56\%$).
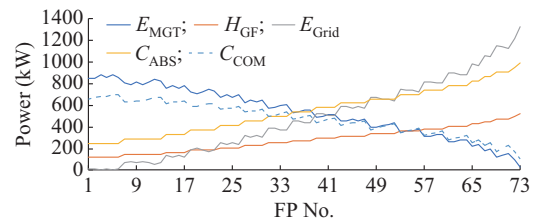

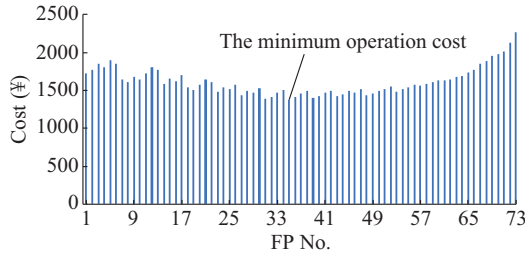Fig 7.   Operation power of components in the 251st interval.

Fig. 8.   Operation cost of system in the 251st interval.

V. STATISTIC RESULTS

In this section, the statistic results of the traditional and the proposed optimization are contrasted. The traditional optimization uses GA (without PFC models) [1], [9], [13] and the proposed optimization uses the FZA method (with PFC models) to find an optimal $K\%$ and its corresponding results, respectively. The two optimizations share the same constraints, power balance equations, objective functions, and the PSR Kalman filter data.

The dispatch schedules of each component solved by GA and FZA are shown in Appendix A. Both schedules obtain accurate power delivery with small errors (3×10^{-5} W for FZA and 1.7×10^{-5} W for GA, respectively). However, the average power, the standard deviation (STD), and the maximum power of each component are very different. The statistic results solved by GA and FZA are shown in Figs. 9-11.
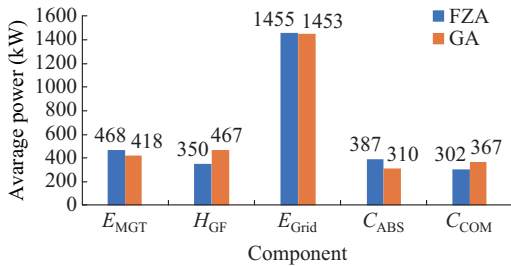

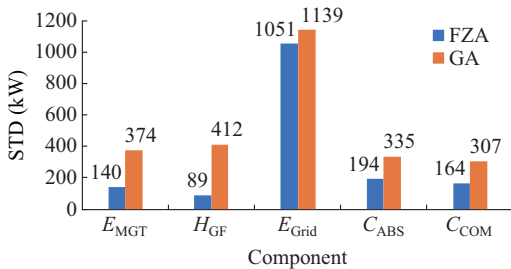Fig 9.   Average power of dispatch schedules solved by GA and FZA.

Fig 10.   STD of dispatch schedules solved by GA and FZA.
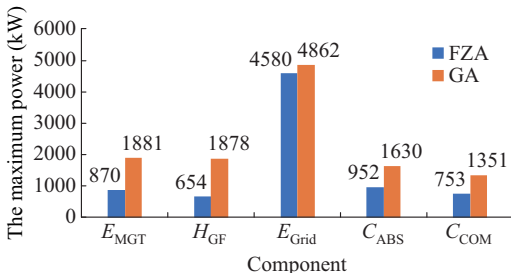

Fig 11.   The maximum power of dispatch schedules solved by GA and FZA.

A. Average Power

Due to the influence of PFC, the power occupation of MGT needs to be higher in order to eliminate the fluctuation caused by GF and ABS. Meanwhile, the MGT is more economical for purchasing electricity or heating generation. Thus, the cost of the proposed optimization is slightly lower than that without PFC models. The power of PFC models is assumed to be between 1% and 5% of the total system power, which causes approximately 0.67% of the dispatch savings.

B. STD

Without PFC models, much power fluctuation would be neglected so that the system needs additional power to satisfy all the loads. Thus, the STD increases and it is not beneficial to CCHPs, which would cause larger dispatch transient, temperature and pressure variation, and waste of power supply.

C. The Maximum Power

Due to the higher power occupation of MGT, the system makes a higher use of the cogeneration. The lower STD reduces the investment of components as well.

If the power of PFC models are assumed to be between 1% and 5%, the least investment of components would be doubled according to the calculation results in Table II.

TABLE II
RESULTS OF PROPOSED AND TRADITIONAL OPTIMIZATION

Model	Algorithm	Dispatch cost (¥)	Power loss (%)	Investment of components (¥)
PFC	FZA	143410	0	1.40×10^7
Without PFC	GA	144388	0	2.88×10^7

VI. CONCLUSION

Compared with traditional optimization, the proposed optimization has higher power from MGT and ABS, lower power from GF and COM, and similar power from the power grid. The PFC model is an explanation of the interaction among MGT, GF, and ABS. It is obvious that the average power of the three components would be different considering PFC models. The proposed optimization results have significant improvements in the STD and the maximum power.
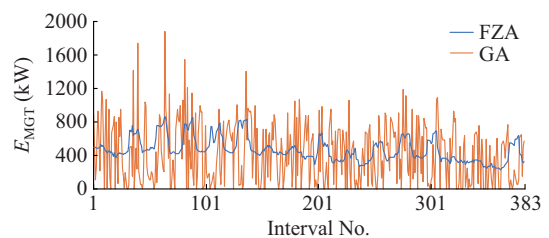
APPENDIX A

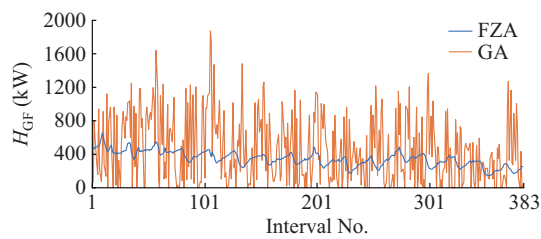Fig. A1.   Electricity from MGT solved by GA and FZA.

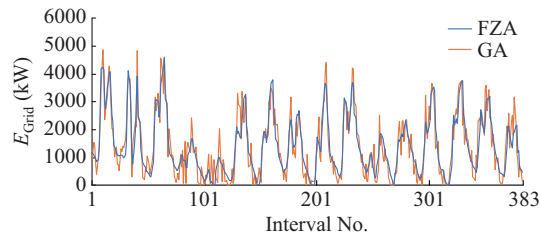Fig. A2.   Heat from GF solved by GA and FZA.

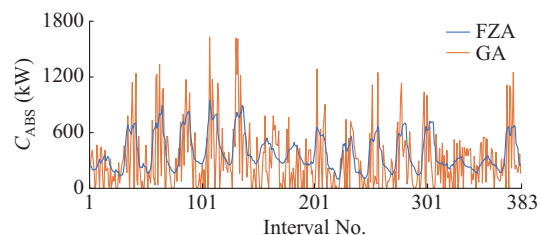Fig. A3.   Electricity from power grid solved by GA and FZA.

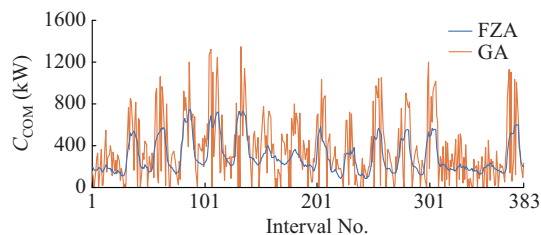

Fig. A4.   Cooling from ABS solved by GA and FZA.

Fig. A5.   Cooling from COM solved by GA and FZA.

REFERENCES

[1] M. Mirzaee, R. Zare, M. Sadeghzadeh *et al*., "Thermodynamic analyses of different scenarios in a CCHP system with micro turbine–absorption chiller, and heat exchanger," *Energy Conversion and Management*, vol. 198, no. 15, pp. 1-15, Oct. 2019.

[2] Z. Wang, H. Li, X. Zhang *et al*., "Performance analysis on a novel micro-scale combined cooling, heating and power (CCHP) system for domestic utilization driven by biomass energy," *Renewable Energy*, vol. 156, no. 1, pp. 1215-1232, Aug. 2020.

[3] Y. Li, R. Tian, M. Wei *et al*., "An improved operation strategy for CCHP system based on high-speed railways station case study," *Energy Conversion and Management*, vol. 216, no. 15, pp. 1-15, Jul. 2020.

[4] O. Sarfraz, C. K. Bach, and C. R. Bradshaw, "Validation of advanced fin-and-tube heat exchanger models with cross-fin conduction functionality," *International Journal of Refrigeration*, vol. 116, no. 1, pp. 70-81, Aug. 2020.

[5] J. A. R. Parise, "Simulation of vapour-compression heat pumps," *Transactions of The Society for Modeling and Simulation International*, vol. 46, no. 2, pp. 71-76, Feb. 1986.

[6] D. Richardson, "An object oriented simulation framework for steady-state analysis of vapor compression refrigeration systems and components," Ph. D. dissertation, Department of Mechanical Engineering, University of Maryland, Maryland, USA, 2006.

[7] S. Saleem, O. Sarfraz, C. R. Bradshaw *et al*., "Development of novel experimental infrastructure for collection of high-fidelity experimental data for refrigerant to air heat exchangers," *International Journal of Refrigeration*, vol. 114, pp. 189-200, Jun. 2020.

[8] J. Wang, H. Zhong, Q. Xia *et al*., "Optimal joint-dispatch of energy and reserve for CCHP-based microgrids," *IET Generation, Transmission & Distribution*, vol. 11, no. 3, pp. 785-794, Jul. 2017.

[9] S. Lu, Y. Li, and H. Xia, "Study on the configuration and operation optimization of CCHP coupling multiple energy system," *Energy Conversion and Management*, vol. 177, no. 1, pp. 773-791, Dec. 2018.

[10] H. Ghaebi, M. Amidpour, S. Karimkashi *et al*., "Energy, exergy and thermoeconomic analysis of a combined cooling, heating and power (CCHP) system with gas turbine prime mover," *International Journal of Energy Research*, vol. 35, pp. 697-709, Jan. 2011.

[11] R. Zeng, H. Li, R. Jiang *et al*., "A novel multi-objective optimization method for CCHP-GSHP coupling systems," *Energy and Buildings*, vol. 112, no. 15, pp. 149-158, Jan. 2015.

[12] L. Li, "Optimization and evaluation of CCHP systems considering incentive policies under different operation strategies," *Energy*, vol. 162, no. 1, pp. 825-840, Nov. 2018.

[13] H. Ershadi and A. Karimipour, "Present a multi-criteria modeling and optimization (energy, economic and environmental) approach of industrial combined cooling heating and power (CCHP) generation systems using the genetic algorithm, case study: a tile factory," *Energy*, vol. 149, no. 15, pp. 286-295, Apr. 2018.

[14] F. Zhao, B. Sun, and C. Zhang, "Cooling, heating and electrical load forecasting method for CCHP system based on multivariate phase space reconstruction and Kalman filter," *Proceedings of the CSEE*, vol. 36, no. 2, pp. 399-406, Feb. 2016.

Pohan Chen received the B.S. degree in Electrical Engineering Department, Harbin Institute of Technology, Harbin, China, in 2013, and M.S. degree in the Department of Electrical Engineering, Tsinghua University, Beijing, China, in 2017. He is currently pursuing the Ph.D. degree in the Department of Electrical Engineering, Tsinghua University. His research interests include the development of multi-energy system and renewable energy microgrid.

Kai Sun received the B.E., M.E., and Ph.D. degrees in electrical engineering from Tsinghua University, Beijing, China, in 2000, 2002, and 2006, respectively. He joined the Department of Electrical Engineering, Tsinghua University, in 2006, where he is currently an Associate Professor. From September 2009 to August 2010, he was a Visiting Scholar with the Department of Energy Technology, Aalborg University, Aalborg, Denmark. From January to August 2017, he was a Visiting Professor with the Department of Electrical and Computer Engineering, University of Alberta, Edmonton, Canada. His research interests include power electronics for renewable generation systems, microgrids, and energy internet.

Chenghui Zhang received the B.E. and M.E. degrees in automation engineering from Shandong University of Technology, Zibo, China, in 1985 and 1988, respectively, and the Ph.D. degree in control theory and operational research from Shandong University, Jinan, China, in 2001. In 1988, he joined Shandong University, where he is currently a Professor with the School of Control Science and Engineering. He is the Chief Manager of Power Electronic Energy-saving Technology and Equipment Research Center of Education Ministry, a Specially Invited Cheung Kong Scholars Professor by China Ministry of Education, and a Taishan Scholar Special Adjunct Professor. His current research interests include renewable energy generation, microgrid, electrical vehicles, complex industrial system optimization and control, research and programming applications.

Bo Sun received the B.S. and Ph.D. degrees from Shandong University, Jinan, China, in 2004 and 2009, respectively. In 2010, he joined Shandong University, where he is currently an Associate Professor with the School of Control Science and Engineering. His current research interests include the optimal control of engineering and the optimization of combined cooling, heating, and power (CCHP) systems.